This is the peer reviewed author accepted manuscript (post print) version of a published work that appeared in final form in:

Wang, Ji, Belusko, Martin, Liu, Ming, Semsarilar, Hesam, Liddle, Raymond, Alemu, Alemu, Evans, Michael, Zhao, Chunrong, Hudson, Julian & Bruno, Frank 2021 'A comprehensive study on a novel transcritical CO2 heat pump for simultaneous space heating and cooling - concepts and initial performance', Energy Conversion and Management vol. 243, article no. 114397, pp. 1-12.

This output may not exactly replicate the final published authoritative version for which the publisher owns copyright. It is not the copy of record. This output may be used for non-commercial purposes. This version is licensed under a Creative Commons CC-BY-NC-ND 4.0 license (http://creativecommons.org/licenses/by-nc-nd/4.0/).

The final definitive published version (version of record) is available at:
https://doi.org/10.1016/j.enconman.2021.114397

Persistent link to the UniSA Research Outputs Repository:
https://hdl.handle.net/11541.2/147922

General Rights
Copyright and moral rights for the publications made accessible in the UniSA Research Outputs Repository are retained by the authors and/or other copyright owners and it is a condition of accessing publications that users recognize and abide by the legal requirements associated with these rights.

- Users may download and print one copy for the purpose of private study or research.
- You may not further distribute the material or use it for any profit-making activity or commercial gain
- You may freely distribute the persistent link identifying the publication in the UniSA Research Outputs Repository

If you believe that this document breaches copyright, please contact us and provide details. We will remove access to the work immediately and investigate your claim.

A comprehensive study on a novel transcritical CO_2 heat pump for simultaneous space heating and cooling - concepts and initial performance

Ji Wang [a*], Martin Belusko [a], Ming Liu [a], Hesam Semsarilar [a], Raymond Liddle [a], Alemu Alemu [b], Michael Evans [c], Chunrong Zhao [d], Julian Hudson [b], Frank Bruno [a]

[a] Future Industries Institute, University of South Australia, Mawson Lakes Campus, Mawson Lakes SA 5095, Australia

[b] Glaciem Cooling Technologies, Mawson Lakes Boulevard, Mawson Lakes SA 5095, Australia

[c] UniSA STEM, University of South Australia, Mawson Lakes Campus, Mawson Lakes SA 5095, Australia

[d] School of Mechanical and Mining Engineering, The University of Queensland, QLD 4072, Australia

Abstract

Carbon dioxide (CO_2) is a natural substance and an environmentally benign, safe and economical refrigerant that can be used for cooling and heating systems. Unlike a traditional reversible heat pump system that only works either in heating or cooling, the air-to-air transcritical CO_2 heat pump system reported in this paper is capable of providing simultaneous space heating and cooling through an Air Handling Unit (AHU) at any time. The system with cooling and heating capacities of 210 kW and 110 kW, respectively, was installed in a cinema complex in South Australia, and continuously operated from September to November in 2020. In this paper, the detailed configuration of the CO_2 heat pump system with parallel compression is described. A complete system layout, comprising of cooling, heating and shared circuits, is revealed for the first time. A mathematical model based on highly efficient Bitzer compressors has also been developed in this study. The experimental data recorded in an entire heating period of approximately one hour has been utilised for model validation and analysis. Through the validation, the simulated power consumption for the compressors with Variable Speed Drive (VSD) and Fixed Speed Drive (FSD) has been compared to the experimental data with acceptable agreements. The simulated discharge temperatures agree with the actual temperatures measured within 10%. Moreover, the latest system performance from September to November has been evaluated based on the heating and cooling loads and combined COPs. It was found that the combined COP was relatively stable at around 3 regardless of climate conditions.

Keywords: transcritical CO_2 system; air-to-air heat pump; simultaneous heating and cooling; mathematical model.

*Corresponding author:

Email address: Ji.wang@mymail.unisa.edu.au,
Jayqinghome@hotmail.com (J. Wang);

Nomenclature

A	Helmholtz Energy	FSD	Fixed Speed Drive
Cp	specific heat capacity, kJ/kg.K	GWP	Global Warming Potential
D	diameter of the bore inside the cylinder, m	HCFC	Hydrochlorofluorocarbon
h	enthalpy, kJ/kg	HFC	Hydrofluorocarbons
L	length of the stroke inside the cyliner, m	ODP	Ozone Depletion Potential
$\dot{m}$	mass flow rate, kg/s	RPM	Revolution Per Minute
n	numbers of the cylinders	sCO_2	Supercritical CO_2
N	rotation speed of the crankshaft, revolutions per minute, rpm	VSD	Variable Speed Drive
P	pressure, bar	***Subscripts***	
Q	heating power, kW	aux	auxiliary
r	compresssion ratio	cool	cooling
T	temperature, °C	comp	compressor
ΔT	temperature difference, K or °C	dem	demand
$\dot{V}$	volumetric flow rate, m^3/s	dis	discharge
V_s	displacement rate of the compressor, m^3/s	ev	evaporation
V_{swept}	volume swept by the piston, m^3	ex	expansion
W_{comp}	compression work, kW	gas	gas cooler
x	vapour mass fraction	heat	heating
Greek symbols		i	numbers of compressors
η	efficiency	in	inlet
η_v	volumetric efficiency of a CO_2 compressor	isentr	isentropic
v	specific volume, m^3/kg	lat	latitude
ρ	density, kg /m^3	long	longitude
Abbreviations		MT	Medium Temperature
AHU	Air Handling Unit	out	outlet
CFC	Chlorofluorocarbon	suc	suction
COP	Coefficient of Performance	super	superheat
FG	Flash-Gas	1 to 10	refrigerants states

1. Introduction

Over the past few decades, environmental problems (such as greenhouse effect and ozonosphere depletion) have deteriorated in-part due to the serious impacts of synthetic refrigerants (e.g. HFC, HCFC and CFC) [1]. A variety of natural refrigerants, therefore, have been considered to replace synthetic chemicals in systems for the purposes of air-conditioning, refrigeration and heat pump [2]. Carbon dioxide (CO_2), also known as R744, is one of the natural substances, which can provide a competitive energy performance with appropriate design [3]. CO_2 is an environmentally benign, safe and economical refrigerant used for heat pump systems. In terms of environmental sustainability, CO_2 is a more promising refrigerant compared with the other five common natural refrigerants (propane, butane, iso-butane, propylene and ammonia). CO_2 has an ODP of zero and GWP of one which is only inferior to ammonia [4]. However, the safety factor also needs to be considered when considering selection, i.e. CO_2 is non-explosive and non-toxic but ammonia is both poisonous and flammable [5]. Additionally, the price of CO_2 refrigerant per unit mass is around three times cheaper than HFC blends (R404A and R407A), according to the latest NCI report [6].

The conventional (or subcritical) CO_2 refrigeration system was first developed in 1850 [7]. The thermodynamic cycle described in *Fig. 1* operates below the critical point of CO_2, i.e. 73.8 bar and 31.1 °C. In a subcritical CO_2 cycle, there is a phase change during the condensation (from state 2' to 3) and the discharge temperature post-compression normally is lower than 80 °C [8, 9]. Therefore, the amount of rejection heat from CO_2 is significantly low in a subcritical cycle, which leads to low heat capacity and relatively low heating efficiency [10]. The transcritical CO_2 cycle is then introduced, in which the gas cooling process (or condensation) occurs beyond the critical pressure, in order to deliver a higher heat rejection enthalpy [11], as shown in *Fig. 2*. In a transcritical condition, heat rejected from the gas cooling process can be utilized for various heating applications, e.g. water heating, space heating, dehumidifying, and food processing [12, 13]. In regards to the transcritical CO_2 heat pump water heater, it has been investigated by many researchers for various purposes of potable water heating [14-16], sanitary water heating [17], general water heating [18, 19], and high-temperature water heating [20]. Also, CO_2 heat pump systems with the combinations of water heating and space heating have been developed and investigated by some researchers [21-23]. Additionally, a prototype of a transcritical CO_2 heat pump dryer with operating temperatures between -20°C and 90°C, and the upper-pressure limit of 130 bar, was developed and utilised for drying different material products [24].

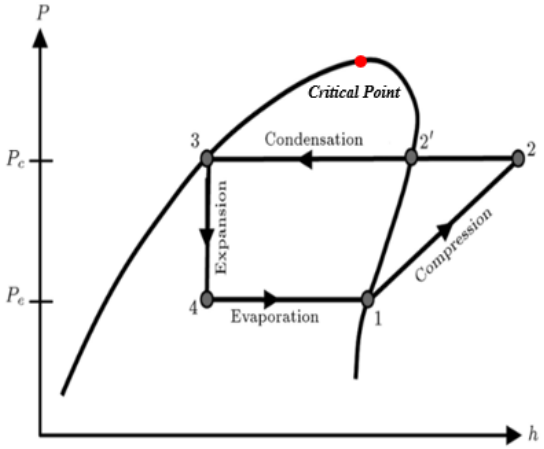


Figure 1 The P-h cycle of a conventional CO_2 system

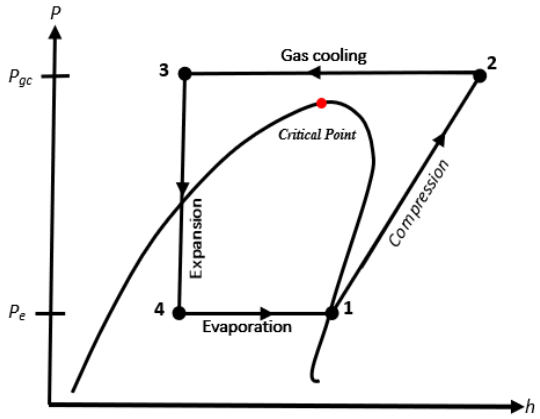


Figure 2 The P-h cycle of a transcritical CO_2 system

A wealth of research has focused on heat pump systems for simultaneous heating and cooling using HFC and natural refrigerants, due to the main advantages of energy input reductions and capital cost savings [25, 26]. The majority of existing systems still need to heat or chill the water through heating or cooling coils first, and then the water can be utilised for multiple purposes. A transcritical CO_2 heat pump in a dairy plant, which was capable of providing warm and chilled water simultaneously has been studied by Sarkar et al. [27]. Water at room temperature was supplied as the heat exchange fluid during the gas cooling and evaporation processes, in which the warm water at the gas cooler outlet was maintained at 73 °C and the chilled water was around 4°C at the evaporator outlet. It should be noted that the correlations of the volumetric efficiency and isentropic efficiency estimated from Ortiz et al. were employed to describe the performance of the semi-hermetic compressor in the system [28]. Another heat pump system using two refrigerants (HFC R407C and CO_2) for simultaneous space heating and cooling, which was designed for office buildings, hotels, and dwellings has been investigated by Byrne et al [29]. Water in two tanks were chilled and heated through the evaporator and the condenser (or the gas cooler), respectively, which was then used to chill and heat the air for space cooling and heating. The annual simulation revealed that CO_2 is more advantageous in a heat pump system for a larger temperature glide and a larger heat capacity. Another similar study focusing on a low-energy building, office building and retail store has been investigated in 2013 [30]. Three refrigerants, i.e. R407C, R290 and HFO1234yf, were selected for this comparative study. It was found that the system with R290 showed the best seasonal energetic performance. In another study, it was also suggested that small fan-coil units are normally required for space heating and cooling in the case of water [31].

In terms of air-to-air heat pump systems, Zhang et al. had reported an application using the refrigerant R22 to provide heating in the coldest place of China [32]. An ejector expansion transcritical CO_2 system has been developed and studied experimentally by Liu et al. [33]. Based on the performance analysis of a CO_2 rooftop system with an internal heat exchanger conducted by Calabrese et al [34], it was concluded that the heating COP was less than or equal to that of the system with HFC when the air temperature at the gas cooler inlet is higher than 16°C. However, there are few studies in the literature investigating the daily combined performance of air-to-air CO_2 heat pumps for simultaneous heating and cooling with long-term operation. In other words, even the heating performance with CO_2 was known to have a relatively poor COP. The combined performance (including heating and cooling) for an air-to-air CO_2 heat pump is an area with limited research.

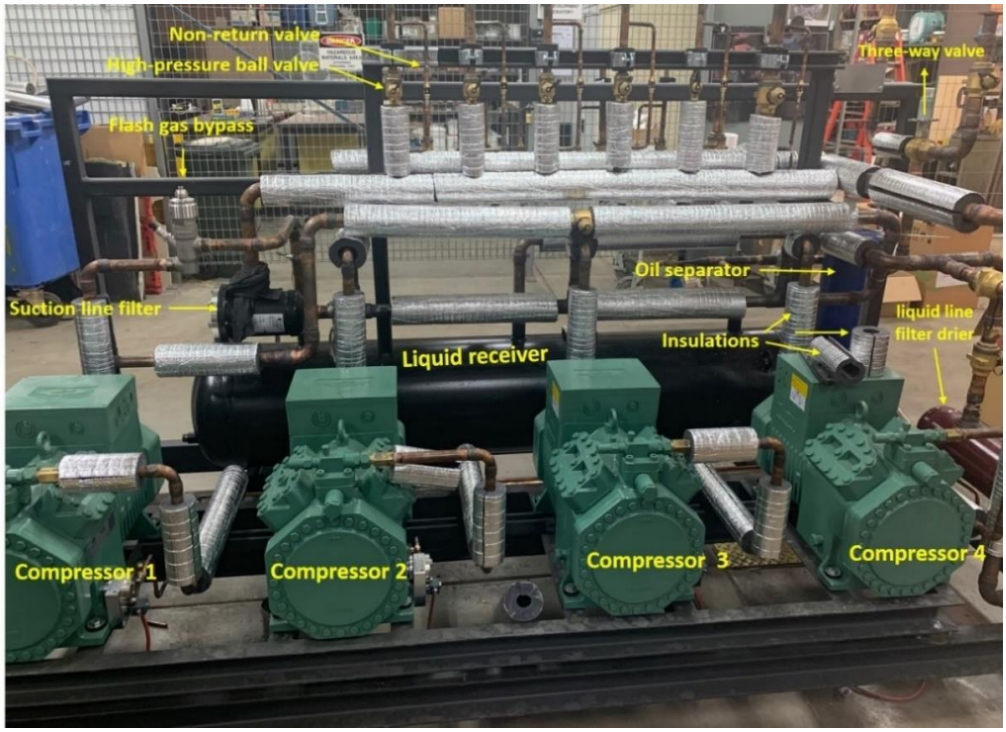
In this study, unlike a traditional reversible heat pump system that only works either in heating or cooling or requires the water loop, the proposed air-to-air CO_2 heat pump is capable of providing simultaneous space heating and cooling directly through the AHU at any time. The detailed configuration of a CO_2 heat pump system with parallel compression is reported. It presents the CO_2 system layout designed for simultaneous space heating and cooling in a cinema. A validated mathematical model with

highly efficient Bitzer compressors is developed and discussed. Additionally, system performance on simultaneous heating and cooling over three months of operation is compared, analysed and evaluated.

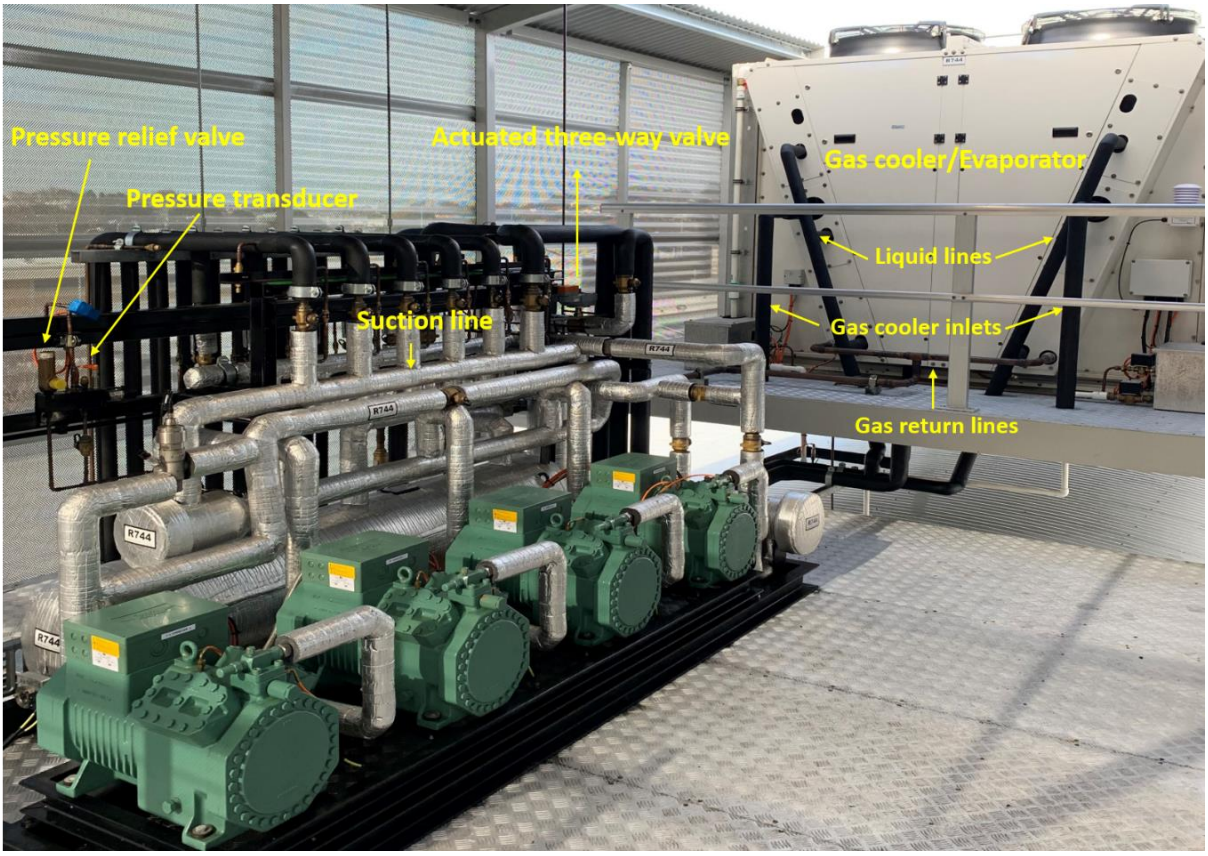
2. Configuration Description

The CO_2 heat pump system with parallel compression, as shown in *Fig. 3*, is able to provide three modes across four seasons, i.e. heating only, cooling only and simultaneous heating and cooling. The cooling and heating capacities designed for the system are 210 kW and 110 kW respectively. The whole system is comprised of several components with the consideration of heating and cooling loads required in the cinema, e.g. four compressors, a gas cooler (or an evaporator), a liquid receiver, and different types of valves. In the CO_2 system (see *Fig.3(a)*), three compressors operate in a row within the medium-temperature cycle, in which compressor 1 runs with variable speed drive (VSD) depending on the heating or cooling demand required, while compressor 2 and/or 3 operate with fixed speed drive (FSD). The auxiliary compressor 4 in the parallel cycle also runs with VSD. The gas cooler (or an evaporator) shown in *Fig.3(b)* is a finned-tube heat exchanger with fans, which uses the ambient air to cool down or heat up the refrigerant, releasing the heat during the gas cooling and absorbing the heat during the evaporation. As shown in the figure, the gas cooler inlets and gas return lines are active when the device operates as a gas cooler, while the liquid lines and suctions lines (which are invisible as they were piped inside the device) are active when the device operates as an evaporator. The gas return lines are not insulated as the temperature of gas cooler outlet is similar as the ambient temperature (that is, approximately 25 °C). The liquid receiver is used to separate the mixture of CO_2 liquid and vapour after the throttling process, that is, the saturated vapour will return back to the auxiliary compressor 4 while the saturated liquid will be operated for further expansion. The function of the oil separator is to filter the lubricant oil from the hot gas and then return it back to the oil reservoirs of the compressors. Additionally, both the liquid line filter drier and the suction line filter are utilised for dust and removal of acids.

In terms of different valves in the system, the three-way valve is used to allocate the refrigerant mass flow rate delivering for heating and cooling post-compression, depending on signals from room thermostats. The other function of the three-way valve is to bypass redundant heat through the gas cooler, in order to maintain the discharge pressure not overly high. The function of the flash gas bypass valve is to circulate the pure saturated vapour back to the auxiliary compressor 4 after the vapour-liquid separation. When the refrigerant is at a high-pressurised environment, both the non-return valve and the high-pressure ball valve are combined to direct and control the flow. In addition, a pressure relief valve and the pressure transducer are installed as safety measures.



(a)



(b)

Figure 3 A complete system includes: (a) Major CO_2 equipment and valves (b) An overview

3. System Layout & Thermodynamics Cycles

The detailed CO_2 system layout for providing heating and cooling in a cinema is shown in *Fig.4*. The red line is a fluid circuit when it is active in the heating mode, the blue line is a circuit when it is active in the cooling mode, and the black circuit is a shared circuit for dual modes. The system is able to supply either cooling or heating to all three theatres and one foyer, while the project room only provides cooling at all times. Regarding the valves described in *Table 1*, the expansion valves (V1, V2, V3, V4 and V9) are opened only for cooling, while two-way ball valves (V5, V6, V7 and V8) are turned on only for heating. Another two electronic expansion valves (V10 and V11) are used to drop the fluid pressure during the throttling process, i.e. V10 is turned on when the cooling demand is lower than the heating demand and V11 is switched on when the fluid temperature is lower than the setting temperature. Additionally, the main temperature sensors are also displayed in the Figure.

The CO_2 system with parallel compression which can run to provide simultaneous heating and cooling in a cinema involves four major processes, as described in the following paragraphs. It should be noted that the states pointed out in *Fig.4* are consistent with those in the P-h diagram, as shown in *Fig.5*.

1. Medium-temperature compressors (compressors 1 to 3) operate with a parallel compressor (compressor 4) to heat up CO_2 vapour to a supercritical state, i.e. state 5.

2. Due to a three-way valve (V12) post-compression, there are three possibilities for the refrigerant CO_2 flowing afterwards, i.e. all refrigerant into the cooling circuit, all refrigerant into the heating circuit, and all refrigerant being separated into two circuits. In the heating circuit, hot sCO_2 will be utilised for space heating through heating coils, which indicates the movement from state 5 to 6. In the cooling circuit, sCO_2 will pass through the gas cooler for releasing the heat, which is from state 5 to 6'.

3. After the heat rejection process, the CO_2 fluid from the cooling circuit and/or heating circuit gathers, followed by a throttling process from state 6 (or 6') to 7 via an expansion valve V11. There is a mixture of vapour and liquid entering the liquid receiver, in which two phases of CO_2 is separated physically. Then, the saturated CO_2 vapour coming out of the receiver passes through a flash gas bypass valve to reach compressor 4, which implies the process from state 7 to 3. Concurrently, the amount of saturated liquid separated from the mixture flows out of the receiver, and then passes through the liquid line filter drier, which indicates the movement from state 7 to 8.

4. In terms of the heat injection process, there are two situations involved, i.e. space cooling and absorbing heat from ambient air through the evaporator. When it is for space cooling, the saturated fluid will go through the expansion valve (V1, V2, V3, V4 or V9) to drop the pressure first (from state 8 to 9) and then to provide cooling through cooling coils, which is from state 9 to 10. When the heat is absorbed through the evaporator, the fluid will drop the pressure via the expansion valve V10 first (from state 8 to 9') and then inject the heat from ambient air through the evaporator (from state 9' to 10). It should be noted that when the system is used for simultaneous heating and cooling, V10 will be turned on automatically once the cooling demand is lower than or equal to the heating demand. As the project room is only provided cooling at all times, the function of the Evaporator Pressure Regulator (EPR) is to maintain a constant suction pressure during the evaporation process. Eventually, the suction line filter is used to filter and superheat the suction gas, in order to avoid the liquid strikes for the compressors, i.e. the process from state 10 to 1.

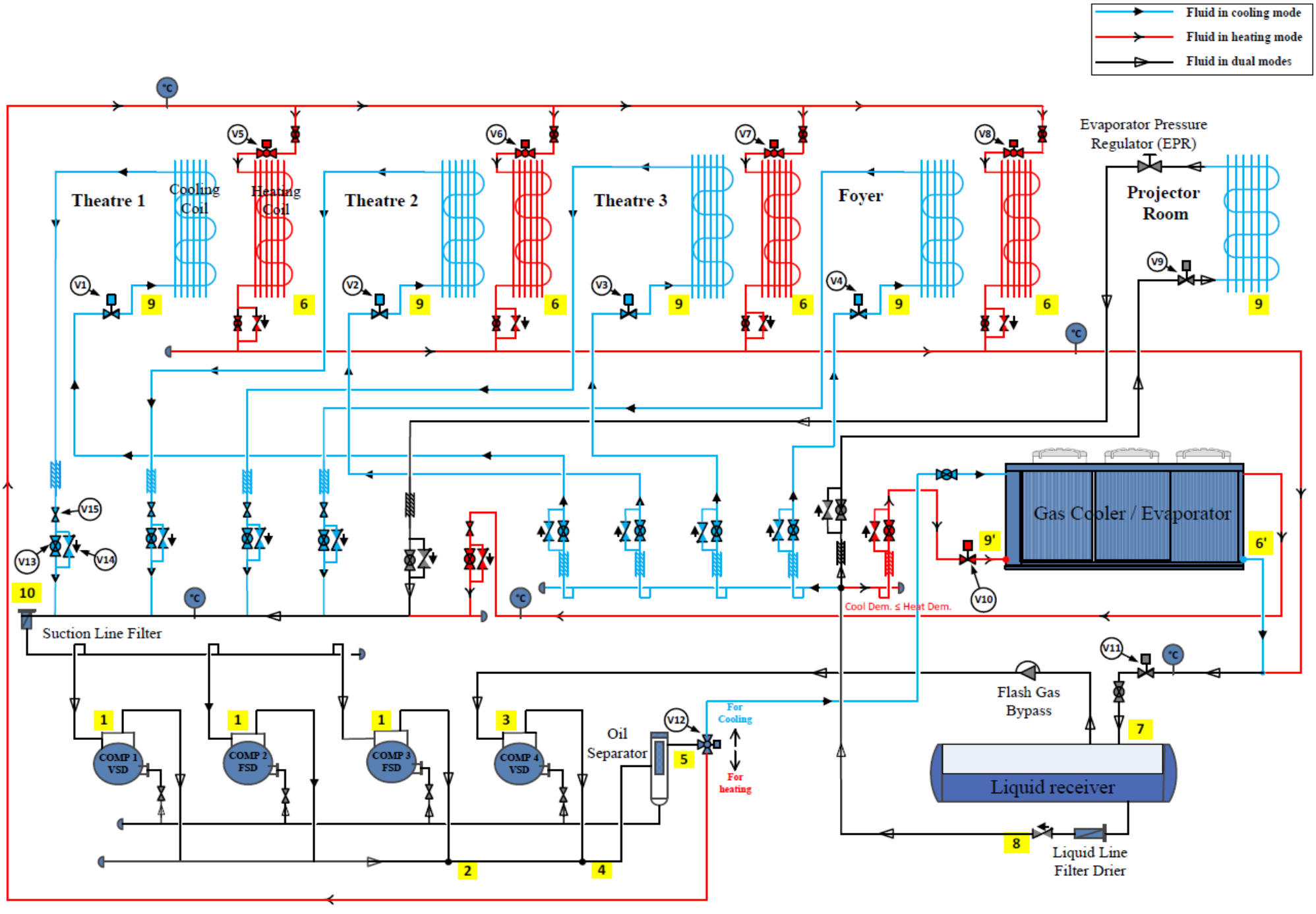


Figure 4 Full schematic layout of the transcritical CO_2 heat pump system installed in the cinema

Table 1. The description of valves used in the system

Displayed Sign	Descriptions
	Electronic Expansion Valve
	2-Way Ball Valve
	3-Way Ball Valve
	High-pressure Ball Valve
	Non-return Valve
	Shut-off Valve

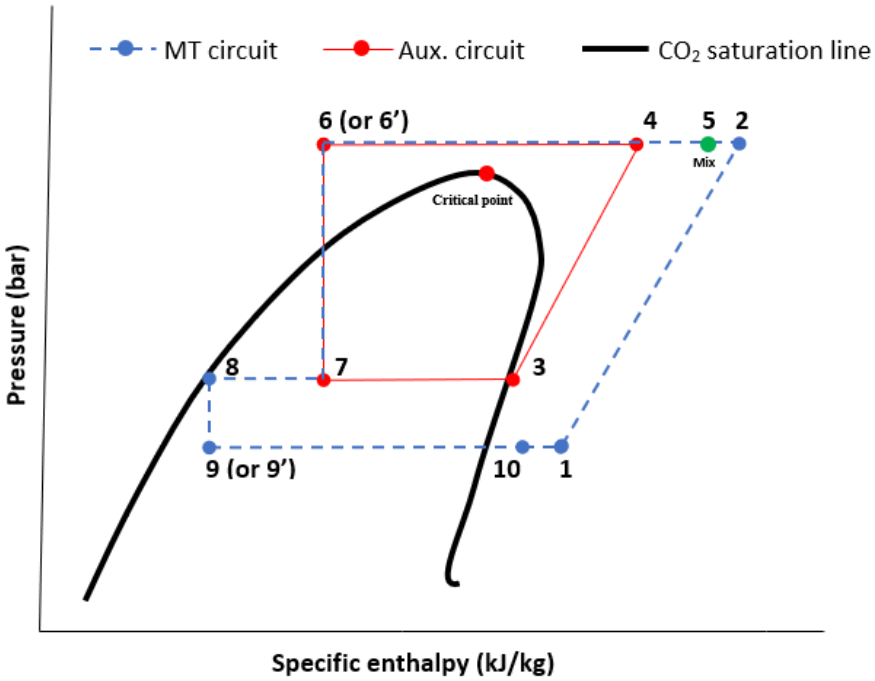


Figure 5 The P-h diagram of CO_2 system with parallel compression

4. Mathematical Modelling

4.1 Model assumptions

The mathematical model of four main components for the transcritical CO_2 heat pump system has been developed. Several assumptions have been made, which include:

1. The system operates at a steady state.
2. The compression work is an adiabatic but not isentropic process.
3. Pressure drop during the gas cooling process is negligible.
4. Heat loss due to friction between the refrigerant and pipe is negligible.
5. All pipes are well-insulated, so heat leakage or loss inside the pipes is negligible.
6. Potential and kinetic energy changes throughout the system are negligible.
7. The process in the expansion valves is isenthalpic.
8. The evaporation temperature (T_{ev}), gas cooler outlet temperature (T_{gas_out}), discharge pressure (P_{dis}) and suction gas superheat (ΔT_{super}) are given as required.

4.2 CO_2 compressor model

The mass flow rate of a single semi-hermetic reciprocating compressor can be defined as:

$$\dot{m}_{comp} = \frac{\eta_v \times V_s}{v_{suc}} \tag{1}$$

where η_v is the volumetric efficiency of the compressor, v_{suc} is the specific volume of CO_2 at the compressor suction state, which depends on the suction gas superheat ΔT_{super} and the evaporation temperature T_{ev}, and V_s is the displacement rate of the compressor which can be calculated from:

$$V_s = \frac{V_{swept} \times N}{60} \tag{2}$$

where N is the rotation speed of the crankshaft and V_{swept} is the volume swept by the piston inside the cylinder, which can be written as:

$$V_{swept} = \frac{\pi}{4} \times D^2 \times L \times n \tag{3}$$

where D is the diameter of the bore inside a cylinder, L is the length of the stroke inside a cylinder, and n is the numbers of the cylinders in the compressor.

In terms of the compressor performance, the compression ratio is defined as the discharge pressure (P_{dis}) over the suction pressure (P_{suc}), that is:

$$r = \frac{P_{dis}}{P_{suc}} \tag{4}$$

In this study, the volumetric efficiency for a semi-hermetic compressor manufactured from Bitzer can be estimated with the function of compression ratio [35], of which correlation is:

$$\eta_v = 1.1785 - 0.1755 \times r + 0.0152 \times r^2 \tag{5}$$

The isentropic efficiency of a Bitzer compressor can be described based on real performance data, which is:

$$\eta_{isentr} = -161.48 + 413.74r - 438.47r^2 + 247.09r^3 - 78.081r^4 + 13.117r^5 - 0.915r^6 \tag{6}$$

Therefore, the energy required for compression work can be calculated from:

$$W_{comp} = \frac{\dot{m}_{comp}(h_{dis,isentr} - h_{suc})}{\eta_{isentr}} \tag{7}$$

where $h_{dis,isentr}$ is a specific enthalpy at the discharge state during an isentropic compression process and h_{suc} is the specific enthalpy at the compressor suction state.

Then, the enthalpy at the discharge state post-compression can be calculated from:

$$h_{dis} = h_{suc} + \frac{W_{comp}}{\dot{m}_{comp}} \tag{8}$$

For a single compressor, the discharge temperature T_{dis} can be worked out once the enthalpy and pressure at the discharge state have been known. The equations with constants for calculating the CO_2 property has been derived by Huang et al. [36]. The simple correlations among pressure, temperature and enthalpy have been defined by Span and Wagner [37]:

$$h(T, P) = A - T\,(\partial A/\partial T)_v - v(\partial A/\partial v)_T \tag{9}$$

where A is the Helmholtz energy and v is the specific volume.

Finally, the total amount of energy required to drive multiple compressors in the system can be described as follows:

$$W_{total} = \sum_1^n W_{comp_i} \tag{10}$$

where i is the numbers of the CO_2 compressors used in the system.

4.3 CO_2 gas cooler model

As multiple compressors will be utilized for parallel compression in a proposed system, the total mass flow rate during the gas cooling process will be:

$$\dot{m}_{gas} = \sum_1^n \dot{m}_{comp_i} \tag{11}$$

The gas cooler inlet temperature at state 5, i.e. the discharge temperature after stream mixing in Fig.5, can be calculated from:

$$T_5 = \frac{T_4\,\dot{m}_{comp_1} + T_2\,(\dot{m}_{comp_2} + \cdots \dot{m}_{comp_i})}{\dot{m}_{gas}} \tag{12}$$

where T_4 is the discharge temperature in an auxiliary circuit and T_2 is the discharge temperature in a medium-temperature circuit.

Due to the fact that heating coils are utilised for space heating in the proposed system, the heat capacity generated during the gas cooling process can be described as:

$$Q_{heat} = \dot{m}_{gas}(1 - \alpha) \times (h_5 - h_6) \tag{13}$$

where h_5 and h_6 are the enthalpies at the inlet and outlet of the gas cooler, respectively, which can be determined based on T_5, T_6 and P_{dis} via Eq. (9) and α is a volume percentage of the refrigerant allocated for rejecting the heat through the gas cooler, which is controlled by the three-way valve.

Finally, the heating COP can be defined as the ratio of heat capacity over the compression work, which is as follows:

$$COP_{heat} = \frac{Q_{heat}}{W_{total}} \tag{14}$$

4.4 CO_2 evaporator model

As the process in the expansion valve is isenthalpic, there is no energy lost during the process (i.e. $h_{\exp_in} = h_{\exp_out}$). In the proposed system, the throttling processes from state 6 to 7 and from state 8 to 9 can be written as follows:

$$h_6 = h_7 \quad (15)$$

$$h_8 = h_9 \quad (16)$$

where h_6 and h_8 are the enthalpies at the expansion valves inlet, while h_7 and h_9 are the enthalpies at the expansion valves outlet.

During the liquid-vapour separation process, the mass fraction of CO_2 vapour returning back to the auxiliary compressor can be calculated from:

$$x = \frac{h_7 - h_8}{h_3 - h_8} \quad (17)$$

Therefore, the liquid collected in the receiver after a further throttling process will provide a cooling effect in rooms (i.e. from state 9 to 10), of which cooling capacity can be described as:

$$Q_{cool} = (\dot{m}_{gas} - \dot{m}_{ev}) \times (1 - x)(h_{10} - h_9) \quad (18)$$

where $\dot{m}_{ev}$ is the mass flow rate of refrigerant passing through the evaporator, which can be calculated from the equation below:

$$\dot{m}_{ev} = \frac{\dot{V}_{air_ev} \times \rho_{air} \times Cp_{air}(T_{out_air} - T_{ambient})}{h_{10} - h_9} \quad (19)$$

where $\dot{V}_{air_ev}$ is the volumetric flow rate of air based on the fan speed of the evaporator, ρ_{air} is the density of the air, Cp_{air} is the specific heat capacity of air, T_{out_air} is the outlet air temperature of the evaporator, and $T_{ambient}$ is the ambient temperature or the inlet air temperature of the evaporator.

Finally, the cooling COP for the parallel compression cycle is given by:

$$COP_{cool} = \frac{Q_{cool}}{W_{total}} \quad (20)$$

For a simultaneous heating and cooling system, the total COP can be calculated as:

$$COP_{total} = COP_{cool} + COP_{heat} \quad (21)$$

4.5 Air-handling unit model

The heating and cooling loads in each space (Q_{heat_air} and Q_{cool_air}) through the AHU can be calculated as:

$$Q_{heat_air} = \dot{V}_{air_AHU} \times \rho_{air} \times Cp_{air}(T_{supply_air} - T_{return_air}) \quad (22)$$

$$Q_{cool_air} = \dot{V}_{air_AHU} \times \rho_{air} \times Cp_{air}(T_{return_air} - T_{supply_air}) \quad (23)$$

where $\dot{V}_{air}$ is the volumetric flow rate of air through the air-handling unit, and T_{return_air} and T_{supply_air} are the air return temperature and air supply temperature, respectively.

5. Validation

The mathematical model has been validated by comparing the predicted compressor power consumption, discharge temperatures and heat capacity with measured data from the transcritical CO_2 heat pump system installed at the cinema. The experimental data recorded every 30 seconds for the entire heating period from 9.07 am to 9.51 am on 12th September of 2020 are reported in the *Appendix*, where compressor power consumption, temperatures and pressure in the suction and discharge states are listed in *Part A*, while air supply and return temperatures , on/off signals (1 for on and 0 for off) and three-way valve positions are displayed in *Part B*.

During the data collections period of September to November, two compressors were operating in a medium-temperature cycle, i.e. compressor 1 operated from the beginning to the end while compressor 2 joined from the middle of the time depending on the simultaneous changes in heat load. The type of the compressor used in the system was 4HTE-20K, which is a semi-hermetic reciprocating compressor manufactured by Bitzer. Some technical data for the compressor at 50Hz is given as the revolution speed is 1450 RPM and the cylinder dimension is 4 x 34mm x 38mm. Compressor 1 operated with the VSD ranging from 30 to 60 Hz, while compressor 2 operated with a FSD of 50 Hz. The discharge pressure increased gradually from 53.32 bar to 84.5 bar during the period. The power consumption for a compressor changed with conditions at the suction and discharge states (T_{suc}, P_{suc}, v_{suc} and P_{dis}).

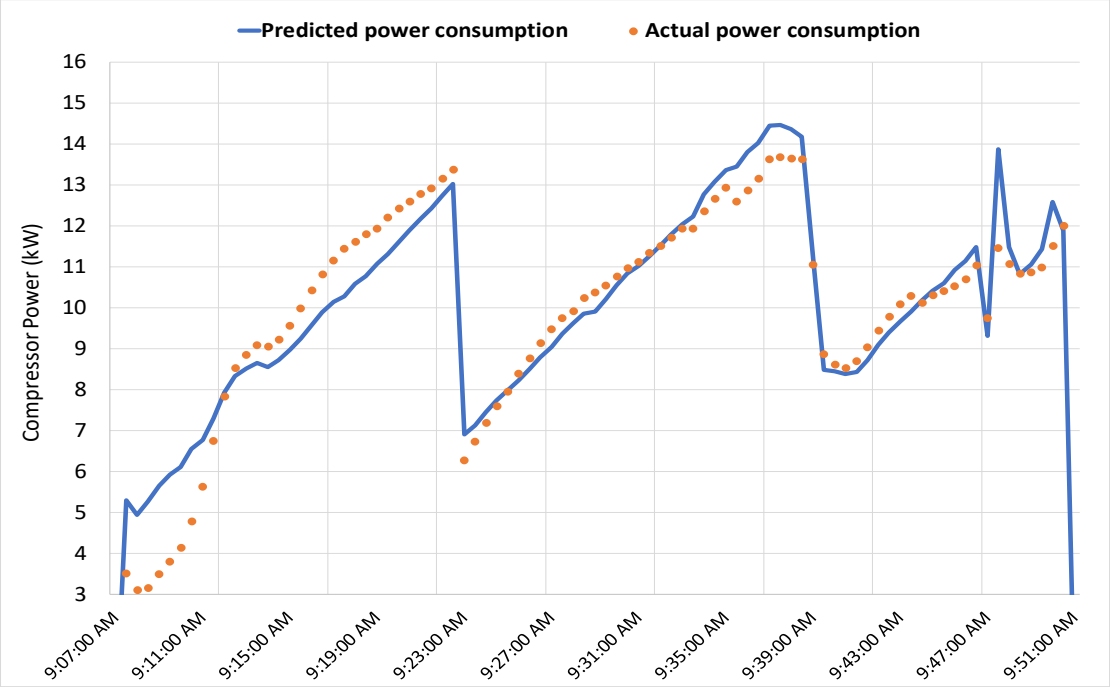


Figure 6 Predicted and measured power consumption for the compressor with VSD

The predicted and actual power consumptions for compressor 1 with VSD and compressor 2 with FSD are displayed in *Fig.6* and *Fig.7* respectively, and the error analysis for these two compressors is displayed in *Fig.8*. In terms of the compressor with VSD, the results show an acceptable agreement with most errors within ±10%. But the simulation has the highest errors when the system is warming up, i.e. the actual power consumption is below 6 kW. However, for the FSD compressor, the difference between the predicted power and the actual power is within ±5%, which is more accurate than that of the compressor with the VSD. It can be explained that compressor 1 with the inverters adjusted the frequency constantly based on the local cooling or heating demand, while compressor 2 always ran at a fixed frequency. Overall, the simulation can predict the power consumption for both FSD and VSD compressors with reasonable uncertainties.

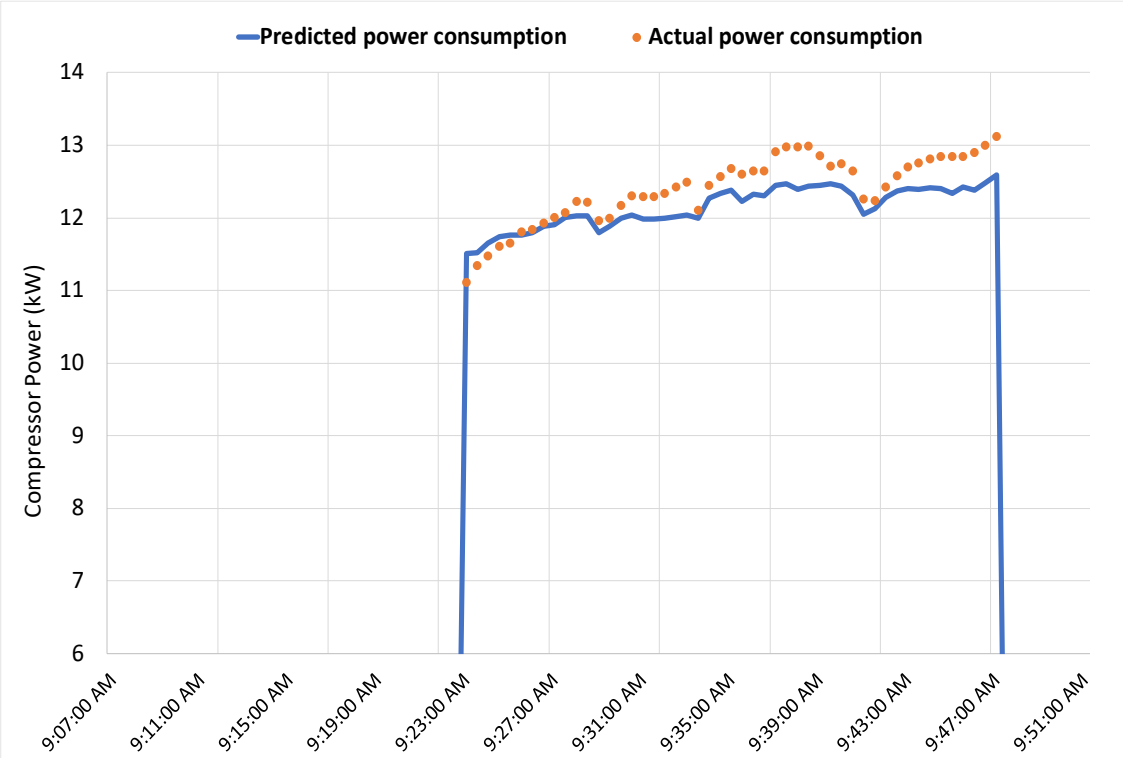


Figure 7 Predicted and measured power consumption for the compressor with FSD

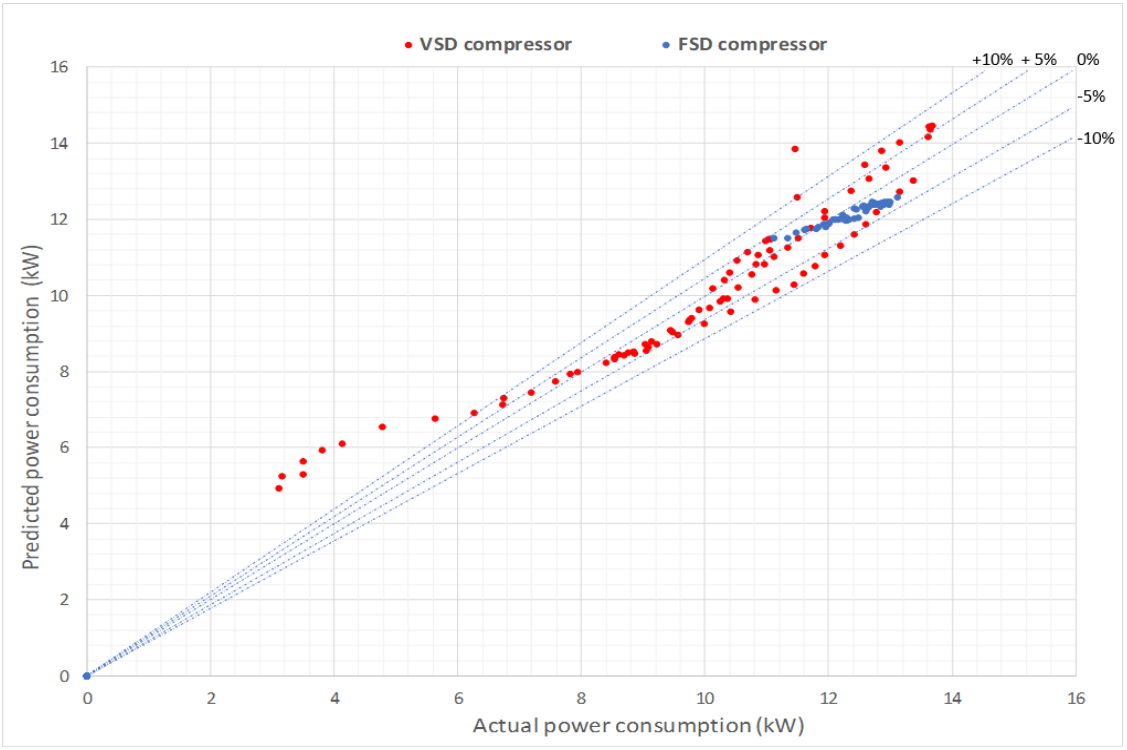


Figure 8 Error analysis of power consumption for compressors with VSD and FSD

The predicted discharge temperatures and the measured coil inlet temperatures have been compared, as described in *Fig. 9*. It shows that the predicted results are always higher than the actual ones with the error less than 10%; even the highest errors occur when the system is warming up in the first few minutes. Theoretically, the discharge temperature post-compression is supposed to be the same as the coil inlet temperature. However, in practice, the heating coils are installed a certain distance apart from the compressor, so it will have some energy losses during the sCO_2 transportation process when the ambient condition is cold, even with the pipes around the heating coils have been relatively well-insulated [38].

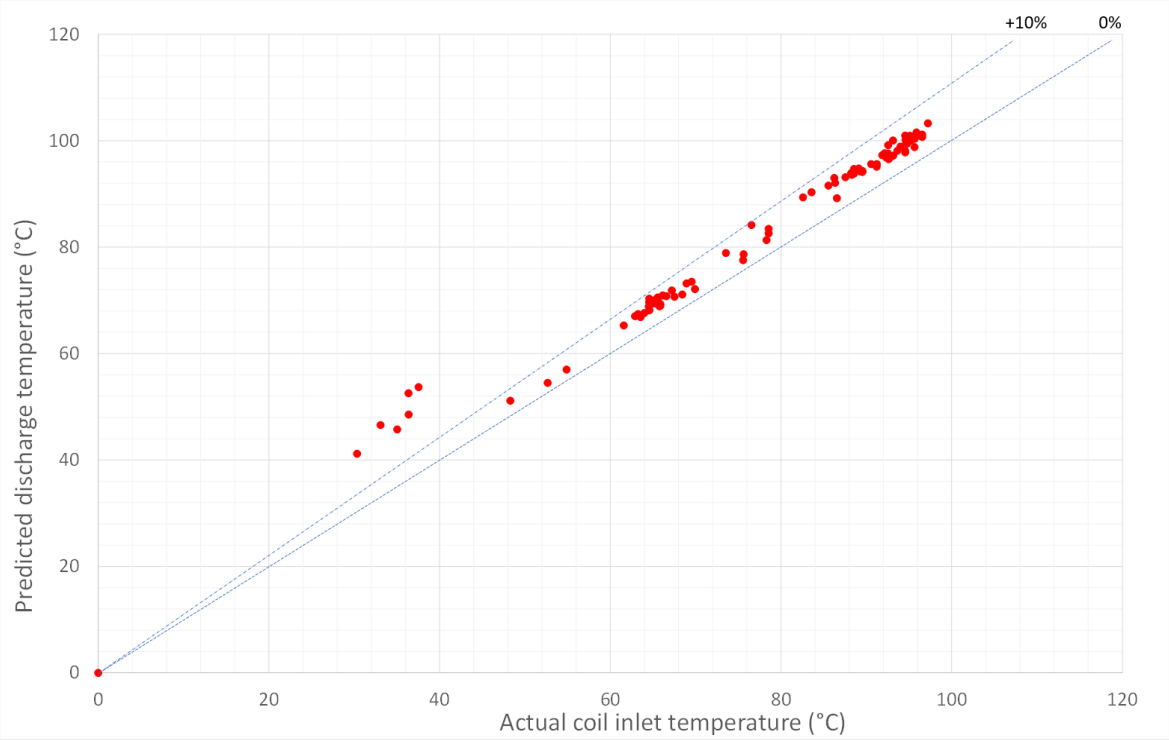


Figure 9 Error analysis of the discharge temperature

Fig.10 displays the predicted heat capacity generated from CO_2 and the actual amount of heat utilised for space heating through the AHU. Several factors have been considered to calculate the heat capacity generated from CO_2, i.e. the calculated mass flow rates, measured inlet and outlet temperatures of the heating coils and the three-way valve positions. The required total heat load is calculated depending on the measured temperatures in each room, i.e. air return and supply temperatures. The air volumetric flow rates for the AHU were measured as 3.17 m^3/s for all the rooms. Some other properties assumed include the density of air is 1.225 kg/ m^3 and the specific heat of air is 1.005 kJ/kg.°C.

As can be seen from the Figure, two curves show a similar trend from 9.14 am to 9.27 am with the error from -2.1% to 18.2%, while there is a big difference between two results during the warming up and the period after 9.27 am. It can be defined that full load indicates that all the rooms are provided heating (except the project room), while full capacity implies that total amount of sCO_2 post-compression entering to the heating circuit but not any fluid passing through the gas cooler (i.e. the three-way valve position is 0%). It can be found that the heat capacity far exceeds the heat demand, when some rooms require no heating between 9.27 am and 9.38 am. However, there were several mismatches between the simulated heat capacity and actual heat load after 9.38 am, when the system is only provided partial heat capacity due to the control of the three-way valve.

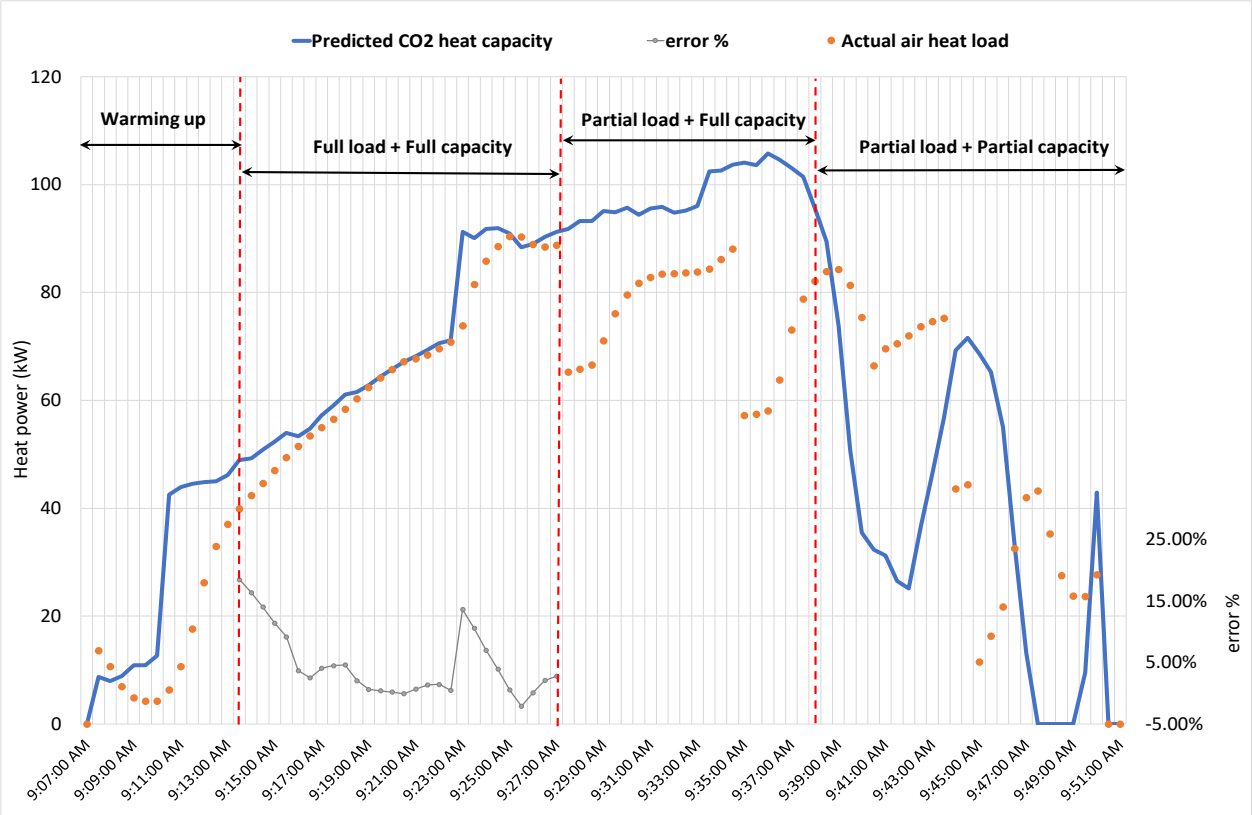


Figure 10 Predicted CO_2 heat capacity Vs. measured air heat load

Fig. 11 shows the error distribution between the CO_2 heat capacity and air heat load. It can be seen that the majority of errors are within the range from -20% to +20%, while the other errors are still very large. The heat capacity can only be verified when the system is at full capacity and full load. The three-way valve in this system did not operate as well as designed. Ideally, the three-way valve was considered to change the valve position consistently and promptly (i.e. to control the mass flow rate in the heating circuit), in order to make the generated heat capacity always meet the needs of the heat loads. However, in practice, the valve positioning takes time during the partial load. The delayed response to the variation of the heat load resulted in an abnormal heating process (e.g. from 9.39 am to 9.44 am in Fig. 10) and led to a significant error being predicted by the model, while the factor of delay-time is not accounted for in the simulation.

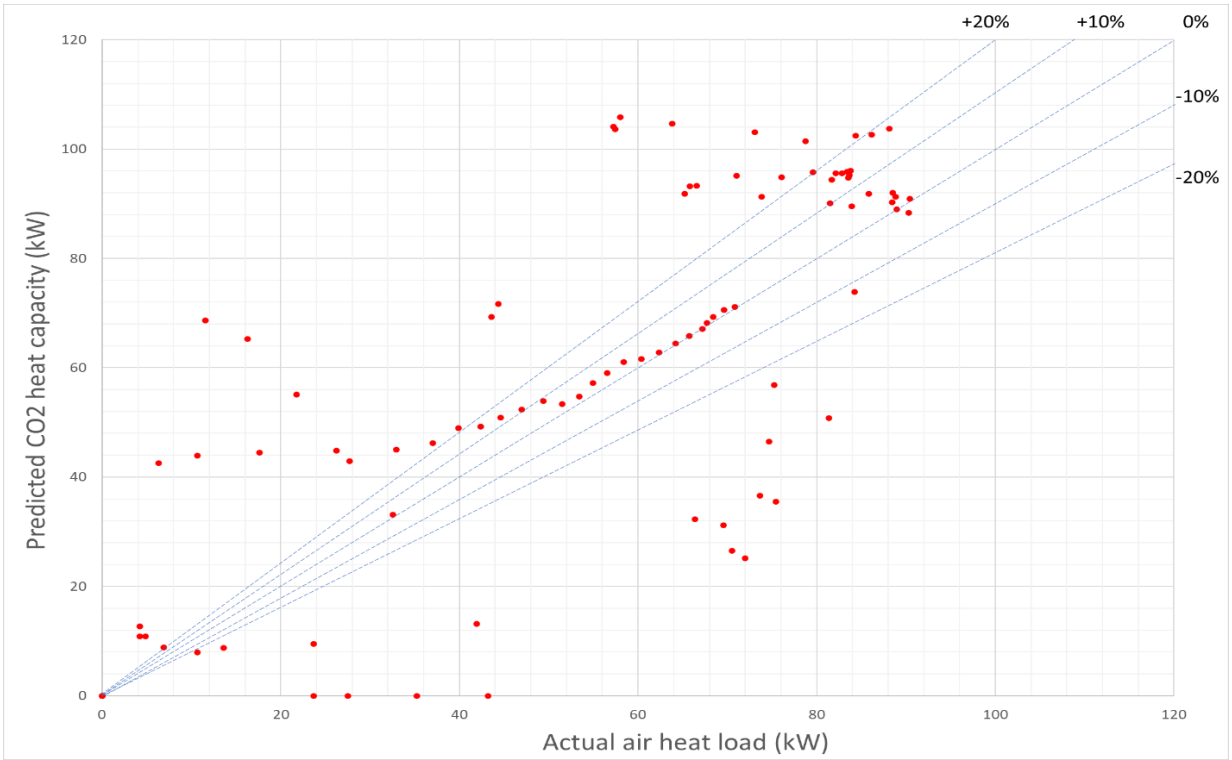


Figure 11 Error analysis for CO_2 heat capacity and air heat load

In addition, cooling capacity is not validated based on the actual cooling loads provided to the project room in the dominant heating mode, as some amount of heat can be absorbed from ambient air through the evaporator but the outlet air temperatures were not measured at that time. Alternatively, the cooling capacity can be validated in the dominant cooling mode, in which the cooling capacity will be equivalent to the total cooling loads provided to all the rooms.

6. Performance Overview

The complete CO_2 system with AHU was set up and came into operation in a cinema at Mount Gambier, South Australia (Lat.: 37.83°S, Long.: 140.78°E) since September 2020. The latest results on the system performance over the past three months has been recorded and utilised for comparison. September, October and November in spring are three transition months in Mount Gambier, in which the morning and evening temperatures are as low as that in winter while the daytime high-temperatures can be as high as in summer [39]. It is possible for a system to provide both heating and cooling throughout the same day, with the variation of ambient temperatures. It should be noted that the days without heating or cooling loads are the closed days of the cinema, e.g. 7th, 14th and 21st of September.

Actual heating & cooling loads and ambient weather conditions (i.e. maximum and minimum ambient temperatures) on a daily basis are shown in *Fig. 12* [40]. It can be seen that September had most of the days with dominant heat loads, while November had several days with dominant cooling loads. There is little difference between daily heating and cooling loads in October, due to small ambient temperature differences. Statistically, the daily energy consumption for heating and cooling in these three months are calculated as 184.97 kWh_{heat} and 140.12 kWh_{cool} in September, 123.49 kWh_{heat} and 140.75 kWh_{cool} in October, and 32.19 kWh_{heat} and 169.97 kWh_{cool} in November. It can be explained that the energy consumption for heating and cooling are affected not only by the real ambient temperatures but also it depends on the actual operating time of heating and cooling in each room. Due to the cold weather in September and October, all three theatres and the foyer were provided space heating for most of the time, except that Theatre 3 and foyer were provided space cooling on the 19th and 20th of September and all three theatres and foyer were supplied cooling on the 2nd and 3rd of October. It should be noted that the project room is only provided cooling and the AHU runs as long as the system is on. Moreover, the dominant demand for most of the days in November is for cooling which is due to warm weather conditions.

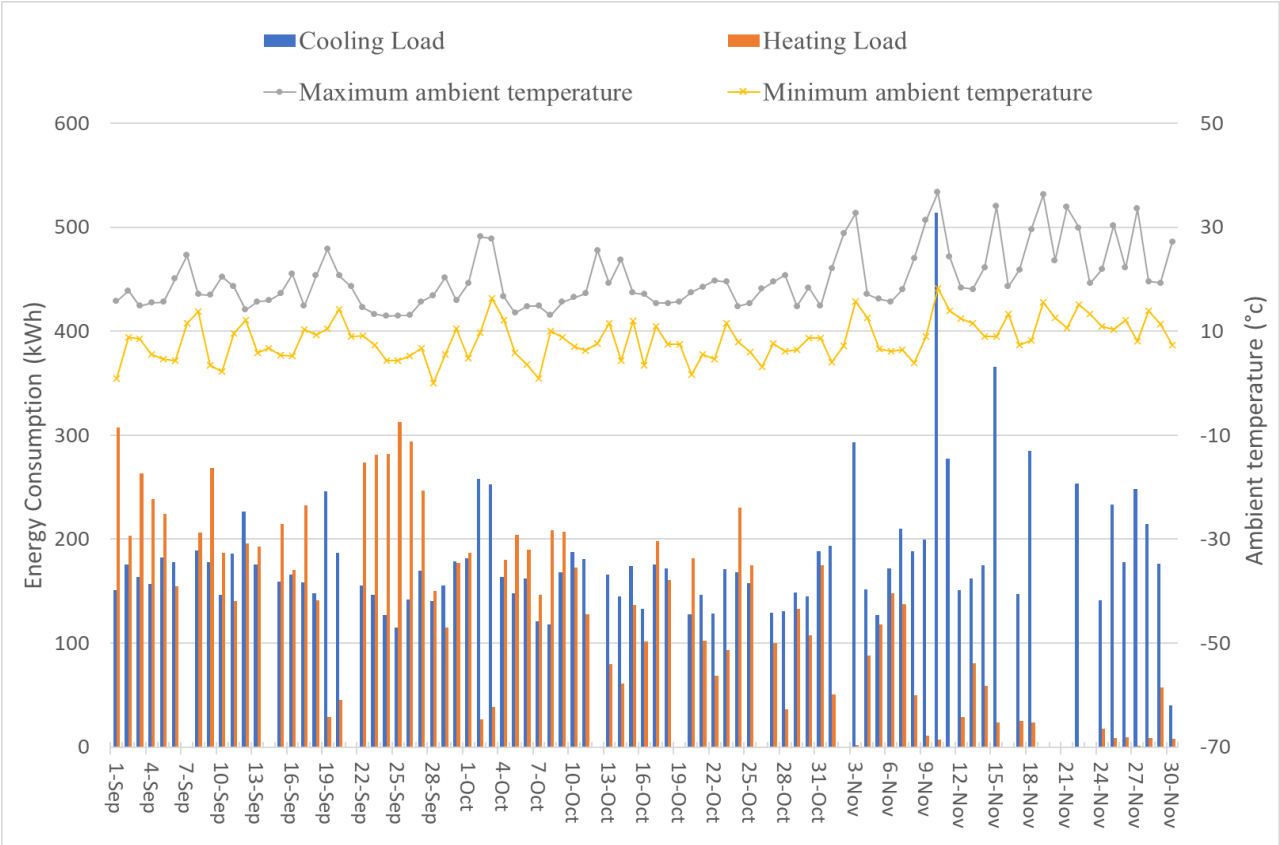


Figure 12 Daily cooling and heat loads of the CO_2 heat pump from September to November

In terms of daily combined COPs from September to November, as shown in *Fig. 13*, the average COP is around 3.27. It can be concluded that the system COP is relatively stable at around 3 regardless of the real weather conditions, which can be used to demonstrate the advantages of the simultaneous heating and cooling systems. The variation of the COPs is relative to the compressor power consumption and useful loads for space heating and cooling based on the actual demands.

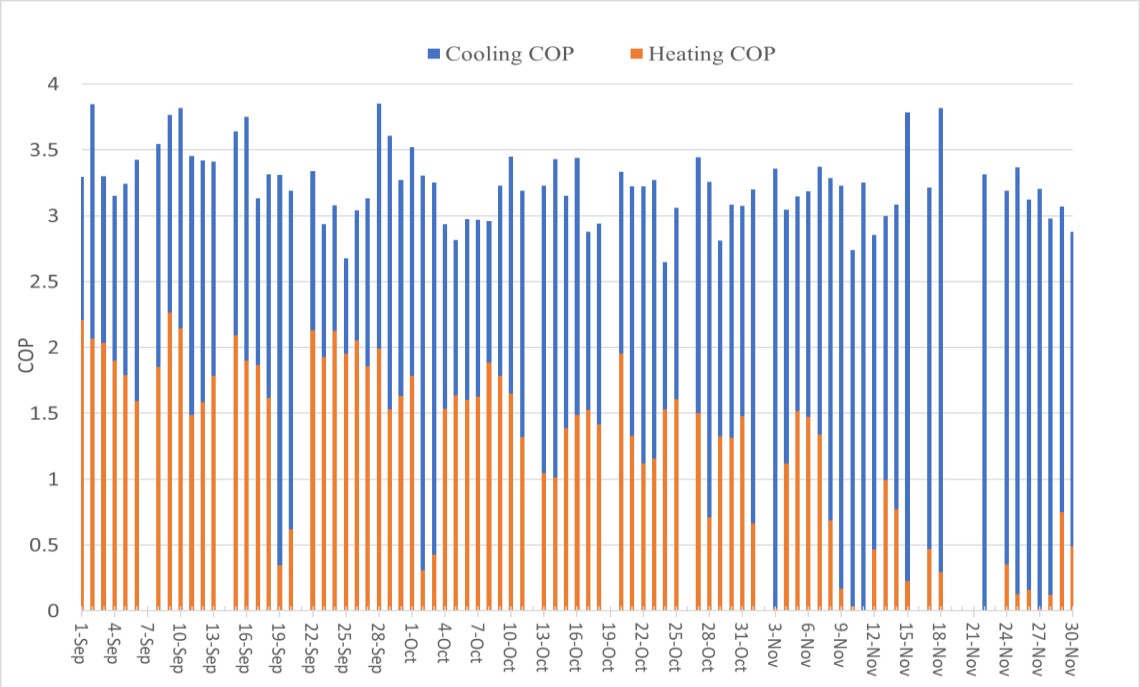


Figure 13 Daily system efficiency of the CO_2 heat pump from September to November

The performance of the CO_2 system has been compared with those of a system using HFC (R407) conducted by Byrne et al [26]. The heating only mode in the CO_2 system indicates a situation when three theatres and one foyer are only provided heating within a day, as the project room is only provided cooling at all time. The other two COPs, i.e. COP in cooling only mode and combined COP in simultaneous heating and cooling mode, are also included. The average COPs for both two systems have been used for comparison, as shown in *Fig.14*.

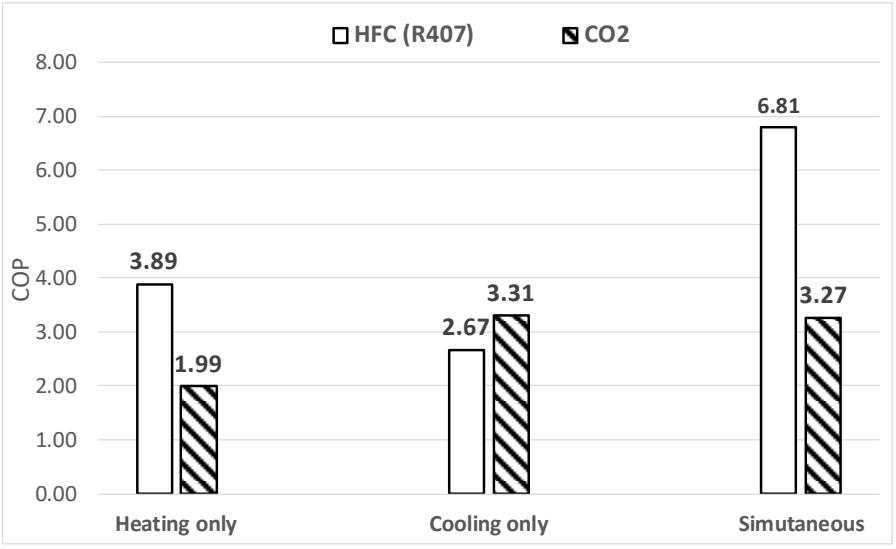


Figure 14 COP comparison between the HFC system and the CO_2 system

Based on the current status, the HFC system with water tanks outperforms the air-to-air CO_2 system in the simultaneous mode and heating only mode. The cooling COP from the CO_2 system is higher. It can be explained that the HFC system stores the majority of rejection heat during the condensation by using the water tank, while there is considerable energy wasted during the air heating process for an air-to-air CO_2 system. Also, as mentioned in the validation part, the current control of the three-way valve led to an abnormal system operation, due to a slow response in valve positioning. Therefore, the heating COP can be further improved once the control of the three-way valve has been optimised.

7. Conclusion

The transcritical CO_2 heat pump system which is capable of providing simultaneous space heating and cooling has been introduced. The following conclusions can be drawn from the study:

- A detailed configuration of a CO_2 heat pump system with parallel compression is described in this study. The complete system layout, comprising of cooling, heating and shared circuits, has been revealed for the first time.

- A mathematical model with a highly efficient Bitzer compressor has been developed. In the compressor model, new correlations for the volumetric efficiency and isentropic efficiency with the function of compression ratio have been developed. The experimental data recorded from an entire heating period has been utilised for validation and analysis. Through comparison, the compressor power consumption with VSD and FSD has been validated against the experimental data and the simulated errors for both compressors were found to be within ± 10 %. The discharge temperatures have also been validated against the actual coil inlet temperatures with acceptable agreements.

- The heat capacity can only be verified when the system is at full capacity and full load, as the three-way valve takes time to move in position during partial load. The delayed response to the variation of the heat load resulted in an abnormal heating process and led to a significant error in the model, while the factor of delay-time is not accounted in the simulation.

- The real system performance from September to November has been evaluated based on the heating and cooling loads, as well as heating, cooling and combined COPs. The daily combined COPs range from 2.64 to 3.85 and the average COP is around 3.27. It was calculated that the COP of heating only mode is around 1.99, while the COP of cooling only mode is 3.31. The system COP is relatively stable at around 3 regardless of the weather conditions, which can be used to demonstrate the advantages of the simultaneous heating and cooling systems.

In future work, a detailed optimisation study on the three-way valve for improving the heating performance of the current system will be conducted. The optimisation study aims to experimentally demonstrate this COP increase.

Acknowledgement

The authors would like to acknowledge the Australian Government for the Research Training Program (RTP) scholarship. The authors would also like to thank Glaciem Cooling Technologies for their industrial support and resources provided.

Reference

1. Nekså, P., *CO2 heat pump systems.* International Journal of Refrigeration, 2002. **25**(4): p. 421-427.
2. Bamigbetan, O., T.M. Eikevik, P. Nekså, and M. Bantle, *Review of vapour compression heat pumps for high temperature heating using natural working fluids.* International Journal of Refrigeration, 2017. **80**: p. 197-211.
3. Lorentzen, G., *Revival of carbon dioxide as a refrigerant.* International Journal of Refrigeration, 1994. **17**(5): p. 292-301.
4. Chaichana, C., L. Aye, and W.W.S. Charters, *Natural working fluids for solar-boosted heat pumps.* International Journal of Refrigeration, 2003. **26**(6): p. 637-643.
5. Maina, P. and Z. Huan, *A review of carbon dioxide as a refrigerant in refrigeration technology.* South African Journal of Science, 2015. **111**: p. 01-10.
6. Bruno, F., M. Belusko, and E. Halawa, *CO2 Refrigeration and Heat Pump Systems—A Comprehensive Review.* Energies, 2019. **12**(15): p. 2959.
7. Ma, Y., Z. Liu, and H. Tian, *A review of transcritical carbon dioxide heat pump and refrigeration cycles.* Energy, 2013. **55**: p. 156-172.
8. Llopis, R., C. Sanz-Kock, R. Cabello, D. Sánchez, and E. Torrella, *Experimental evaluation of an internal heat exchanger in a CO2 subcritical refrigeration cycle with gas-cooler.* Applied Thermal Engineering, 2015. **80**: p. 31-41.
9. Ghazizade-Ahsaee, H. and I. Baniasad Askari, *The application of thermoelectric and ejector in a CO2 direct-expansion ground source heat pump; energy and exergy analysis.* Energy Conversion and Management, 2020. **226**: p. 113526.
10. Bellos, E. and C. Tzivanidis, *A comparative study of CO2 refrigeration systems.* Energy Conversion and Management: X, 2019. **1**.
11. Kim, M.H., J. Pettersen, and C.W. Bullard, *Fundamental process and system design issues in CO2 vapor compression systems.* Progress in Energy and Combustion Science, 2004. **30**(2): p. 119-174.
12. Fricke, B., S. Zha, V. Sharma, and J. Newel, *Laboratory evaluation of a commercial CO2 booster refrigeration system.* 2016.
13. Rony, R.U., H. Yang, S. Krishnan, and J. Song, *Recent Advances in Transcritical CO2 (R744) Heat Pump System: A Review.* Energies, 2019. **12**(3): p. 457.
14. Nekså, P., H. Rekstad, G.R. Zakeri, and P.A. Schiefloe, *CO2-heat pump water heater: characteristics, system design and experimental results.* International Journal of Refrigeration, 1998. **21**(3): p. 172-179.
15. Cecchinato, L., M. Corradi, E. Fornasieri, and L. Zamboni, *Carbon dioxide as refrigerant for tap water heat pumps: A comparison with the traditional solution.* International Journal of Refrigeration, 2005. **28**(8): p. 1250-1258.
16. Saikawa, M. and S. Koyama, *Thermodynamic analysis of vapor compression heat pump cycle for tap water heating and development of CO2 heat pump water heater for residential use.* Applied Thermal Engineering, 2016. **106**: p. 1236-1243.
17. Tammaro, M., C. Montagud, J.M. Corberán, A.W. Mauro, and R. Mastrullo, *Seasonal performance assessment of sanitary hot water production systems using propane and CO2 heat pumps.* International Journal of Refrigeration, 2017. **74**: p. 224-239.
18. Laipradit, P., J. Tiansuwan, T. Kiatsiriroat, and L. Aye, *Theoretical performance analysis of heat pump water heaters using carbon dioxide as refrigerant.* International Journal of Energy Research, 2008. **32**(4): p. 356-366.

19. Qi, P.-C., Y.-L. He, X.-L. Wang, and X.-Z. Meng, *Experimental investigation of the optimal heat rejection pressure for a transcritical CO2 heat pump water heater.* Applied Thermal Engineering, 2013. **56**(1): p. 120-125.
20. White, S.D., M.G. Yarrall, D. Cleland, and R. Hedley, *Modelling the performance of a transcritical CO2 heat pump for high temperature heating (Reprinted).* Int. J. Refrig.-Rev. Int. Froid, 2002. **25**(4): p. 479-486.
21. Stene, J., *Residential CO2 heat pump system for combined space heating and hot water heating.* International Journal of Refrigeration, 2005. **28**(8): p. 1259-1265.
22. He, Y.-J., J.-H. Cheng, M.-M. Chang, and C.-L. Zhang, *Modified transcritical CO2 heat pump system with new water flow configuration for residential space heating.* Energy Conversion and Management, 2021. **230**: p. 113791.
23. Dai, B., H. Qi, W. Dou, S. Liu, D. Zhong, H. Yang, V. Nian, and Y. Hao, *Life cycle energy, emissions and cost evaluation of CO2 air source heat pump system to replace traditional heating methods for residential heating in China: System configurations.* Energy Conversion and Management, 2020. **218**: p. 112954.
24. Eikevik, T.M., I. Strommen, and O. Alves-Filho. *Heat pump fluidised bed dryer with CO2 as refrigerant–Measurements of COP and SMER*. in *3rd Nordic Drying Conference, Karlstad, Sweden*. 2005.
25. Nguyen, C., C.T. Veje, M. Willatzen, and P. Andersen, *Exergy costing for energy saving in combined heating and cooling applications.* Energy Conversion and Management, 2014. **86**: p. 349-355.
26. Byrne, P., J. Miriel, and Y. Lenat, *Experimental study of an air-source heat pump for simultaneous heating and cooling – Part 1: Basic concepts and performance verification.* Applied Energy, 2011. **88**(5): p. 1841-1847.
27. Sarkar, J., S. Bhattacharyya, and M.R. Gopal, *Simulation of a transcritical CO2 heat pump cycle for simultaneous cooling and heating applications.* International Journal of Refrigeration, 2006. **29**(5): p. 735-743.
28. Oritz, T., D. Li, and E.A. Groll, *Evaluation of the performance potential of CO2 as a refrigerant in air-to-air Air conditioners and heat pumps: system modeling and analysis*. 2003, ARTI, Final Report.
29. Byrne, P., J. Miriel, and Y. Lenat, *Design and simulation of a heat pump for simultaneous heating and cooling using HFC or CO2 as a working fluid.* International Journal of Refrigeration, 2009. **32**(7): p. 1711-1723.
30. Ghoubali, R., P. Byrne, J. Miriel, and F. Bazantay, *Simulation study of a heat pump for simultaneous heating and cooling coupled to buildings.* Energy and Buildings, 2014. **72**: p. 141-149.
31. Dai, B., H. Qi, S. Liu, M. Ma, Z. Zhong, H. Li, M. Song, and Z. Sun, *Evaluation of transcritical CO2 heat pump system integrated with mechanical subcooling by utilizing energy, exergy and economic methodologies for residential heating.* Energy Conversion and Management, 2019. **192**: p. 202-220.
32. Zhang, Y., Q. Ma, B. Li, X. Fan, and Z. Fu, *Application of an air source heat pump (ASHP) for heating in Harbin, the coldest provincial capital of China.* Energy and Buildings, 2017. **138**: p. 96-103.
33. Liu, F., E.A. Groll, and J. Ren, *Comprehensive experimental performance analyses of an ejector expansion transcritical CO2 system.* Applied Thermal Engineering, 2016. **98**: p. 1061-1069.
34. Calabrese, N., R. Mastrullo, A.W. Mauro, P. Rovella, and M. Tammaro, *Performance analysis of a rooftop, air-to-air heat pump working with CO2.* Applied Thermal Engineering, 2015. **75**: p. 1046-1054.

35. Bitzer. *Bitzer online software*. 2019; Available from: https://www.bitzer.de/websoftware/Calculate.aspx?cid=1576028948781&mod=HHK.
36. Huang, F.-H., M.-H. Li, L.L. Lee, K.E. Starling, and F.T.H. Chung, *AN ACCURATE EQUATION OF STATE FOR CARBON DIOXIDE.* Journal of Chemical Engineering of Japan, 1985. **18**(6): p. 490-496.
37. Span, R. and W. Wagner, *A New Equation of State for Carbon Dioxide Covering the Fluid Region from the Triple‐Point Temperature to 1100 K at Pressures up to 800 MPa.* Journal of Physical and Chemical Reference Data, 1996. **25**(6): p. 1509-1596.
38. Bojić, M., M. Miletić, and L. Bojić, *Optimization of thermal insulation to achieve energy savings in low energy house (refurbishment).* Energy Conversion and Management, 2014. **84**: p. 681-690.
39. *Climate Glossary*. Bureau of Meteorology Australian Government]. Available from: http://www.bom.gov.au/climate/glossary/seasons.shtml#:~:text=Spring%20%2D%20the%20three%20transition%20months,months%20June%2C%20July%20and%20August.
40. *Mount Gambier Daily Weather Observations*, B.o. Meteorology, Editor. 2020, Australian Government: http://www.bom.gov.au/climate/dwo/202011/html/IDCJDW5041.202011.shtml.